Draft version February 2, 2008
Preprint typeset using LaTeX style emulateapj v. 6/22/04

arXiv:astro-ph/0501453v1 20 Jan 2005

SPECTRAL SIGNATURES OF GRAVITATIONALLY CONFINED THERMONUCLEAR SUPERNOVA EXPLOSIONS

Daniel Kasen[1,2,3] and Tomasz Plewa[4,5,6]

Draft version February 2, 2008

ABSTRACT

We consider some of the spectral and polarimetric signatures of the gravitational confined detonation scenario for Type Ia supernova explosions. In this model, material produced by an off-center deflagration (which itself fails to produce the explosion) forms a metal-rich atmosphere above the white dwarf surface. Using hydrodynamical simulations, we show that this atmosphere is compressed and accelerated during the subsequent interaction with the supernova ejecta. This leads ultimately to the formation of a high-velocity pancake of metal-rich material that is geometrically detached from the bulk of the ejecta. When observed at the epochs near maximum light, this absorbing pancake produces a highly blueshifted and polarized calcium IR triplet absorption feature similar to that observed in several Type Ia supernovae. We discuss the orientation effects present in our model and contrast them to those expected in other supernova explosion models. We propose that a large sample of spectropolarimetric observations can be used to critically evaluate the different theoretical scenarios.

Subject headings: hydrodynamics – supernovae: general – polarization

1. INTRODUCTION

After decades of study, the mechanism of the explosion of a white dwarf in a Type Ia supernovae remains uncertain (Hillebrandt & Niemeyer 2000). Several of the proposed theoretical models (Arnett 1969; Khokhlov 2001; Reinecke et al. 2002) have failed to produce objects with the energetics and chemical composition compatible with observations (Höflich et al. 2002). These two characteristics are best captured by the so-called delayed-detonation models (Khokhlov 1991; Gamezo et al. 2004; Plewa et al. 2004). In such models, a mild ignition occurs near the center of the accreting, massive white dwarf, and sparks a deflagration (subsonic flame). During the subsequent evolution, a deflagration to detonation (supersonic reactive wave) transition (DDT) takes place.

Despite the promise of the DDT models, it remains unclear how a transition to detonation occurs – in all standard DDT models calculated so far, the detonation was triggered artificially. However, Plewa et al. (2004) have proposed a gravitational confined detonation (GCD) model in which a detonation naturally follows a slightly off-center ignition. In this scenario, the deflagration takes the form of a single bubble, buoyantly rising to the stellar surface. At the bubble's breakout, the surface layers of the star are laterally accelerated and begin sweeping across the stellar surface, converging opposite the breakout point. The subsequent compression of the colliding streams and thermalization of the kinetic energy triggers a detonation. The authors speculate that, as in the standard DDT case, the detonation will consume the remaining fuel, producing an energetic explosion with chemically stratified ejecta. The stability of the GCD is currently the subject of more detailed numerical study.

One of the most striking properties of the GCD model is that the products of the deflagration are brought to the surface of the white dwarf prior to detonation. This material constitutes a small fraction of the stellar mass, and is rich in metals. This compositional "pollution" of the outer stellar layers is reminiscent of a peculiar feature noticed in the spectra of some Type Ia SNe. In a handful of objects, observers have identified a highly-blueshifted Ca II IR triplet absorption (Hatano et al. 1999; Li et al. 2001; Wang et al. 2003; Gerardy et al. 2004), indicating absorbing material moving at velocities $\sim 20,000$ km s^{-1}, much higher than that characteristic of other spectral lines. Given that velocity is proportional to radius in expanding supernova atmospheres, the high-velocity (HV) calcium absorption indicates a component of absorbing material geometrically detached from the bulk of the ejecta. Spectropolarimetry of SN 2001el further showed that the HV absorption was highly polarized, indicating that the absorbing material was distributed aspherically with perhaps a clump-like geometry (Wang et al. 2003; Kasen et al. 2003).

In this letter we demonstrate that the ejecta structure characteristic of the GCD scenario can naturally explain observations of the peculiar HV calcium absorption feature in Type Ia supernovae.

2. METHODS

We studied the post-detonation evolution of the GCD model using a simplified numerical setup in which spherical supernova ejecta runs into an aspherical metal-rich atmosphere. For the supernova ejecta structure, we used the W7 model (Nomoto et al. 1984) with an initial radius of 3×10^8 cm. Around the ejecta, we placed an ellipsoidal metal-rich extended atmosphere representing the bubble of burned material expelled during the GCD breakout. The composition of this material was taken to be the oxygen-burned composition #4 from Table 3

---

[1] Allan C. Davis Fellow, Department of Physics and Astronomy, Johns Hopkins University, Baltimore, MD 21218
[2] Space Telescope Science Institute, Baltimore, MD 21218
[3] Lawrence Berkeley National Laboratory, Berkeley, CA 94720
[4] Center for Astrophysical Thermonuclear Flashes, The University of Chicago, Chicago, IL 60637
[5] Department of Astronomy & Astrophysics, The University of Chicago, Chicago, IL 60637
[6] Nicolaus Copernicus Astronomical Center, Bartycka 18, 00716 Warsaw, Poland

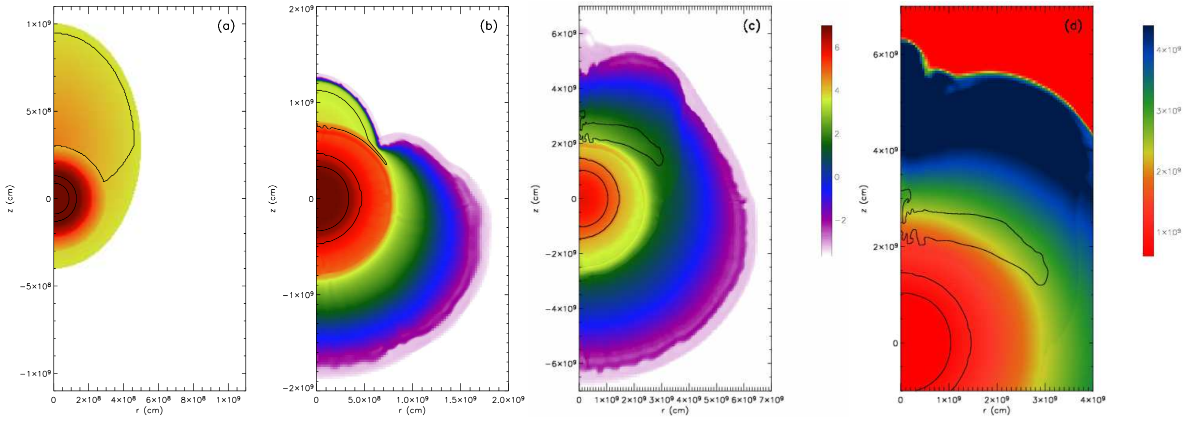

FIG. 1.— Hydrodynamical simulation of the model supernova ejecta interacting with the extended atmosphere. Panels (a)-(c) show the density in log scale; panel (d) depicts the magnitude of the velocity. The density scale is shown by the colorbar in panel (c) while the velocity scale is shown by the colorbar in panel (d). The black contour line corresponds to a calcium number abundance of 0.01. (a) Density distribution at the beginning of the simulation ($t = 0$ s). (b) Density distribution at $t = 0.3$ s. Notice the remarkable deformation of the calcium-rich material in the upper part of the computational domain. (c) Density distribution at the final time ($t = 1.24$ s). Notice that the calcium-rich region has been strongly compressed into a pancake-like structure. (d): Velocity magnitude at the final time. The calcium-rich absorber is seen moving at velocity $\sim 21,000$ km s^{-1} with a substantial velocity gradient across the structure.

of Khokhlov et al. (1993) which consists of 57% silicon, 27% sulfur, 7.1% iron, 2.7% calcium and small amounts of other elements. The extended atmosphere had an axis ratio of 1.2, semi-major axis length of 6×10^8 cm and was centered at 3×10^8 cm. The density of the atmosphere decreased exponentially with a scale length of 3×10^8 cm. The atmosphere was uniformly expanding about its center with velocity proportional to radius and reaching 5000 km s^{-1} at the outer edge. The ejecta and ellipsoidal extended atmosphere were embedded in an ambient medium of pure helium of density 10^{-4} g cm^{-3}. The initial model was isothermal with $T = 10^7$ K. This overall configuration closely represents that seen in the GCD calculations of Plewa et al. (2004).

The hydrodynamic evolution was calculated with the adaptive mesh refinement code FLASH (Fryxell et al. 2000). The initial model was defined on a 2-D cylindrical grid covering the region up to 2.56×10^{10} cm in radius and from -2.56×10^{10} cm to 2.56×10^{10} cm in the z-direction. The ejecta was centered at the origin of the grid. The maximum resolution of the simulation, used only to resolve strong flow structures in the dense regions of the model, was equal to 62.5 km. We used a reflecting boundary condition at the symmetry axis and allowed for free outflow otherwise. We used a Helmholtz equation of state, an iso13 composition (Fryxell et al. 2000), and a multipole solver with 10 terms in the expansion to account for self-gravity.

Spectra of the hydrodynamical models were calculated using a multi-dimensional Monte Carlo radiative transfer code (Thomas 2003; Kasen 2004). The opacities used in the calculation were electron scattering and bound-bound line transitions. Ionization and excitation were computed assuming local thermodynamic equilibrium, where the temperature structure of the atmosphere was determined self-consistently using an iterative approach enforcing radiative-equilibrium (Lucy 1999). Line interactions were treated in the Sobolev approximation and included both absorption and scattering according to a equivalent two level atom scheme with thermalization parameter $\epsilon = 0.01$. Monte Carlo photon packets were initially emitted from a spherical inner boundary surface located at $v = 6000$ km s^{-1} and according to a blackbody distribution with $T = 9000$ K. The packets were initially unpolarized but acquired polarization by electron scattering. Line scattered light was assumed to be unpolarized due to complete redistribution. To construct the emergent spectra and polarization, escaping photon packets were collected into one of 100 angular bins.

3. RESULTS

We have calculated several models assuming different mass of the extended atmosphere. Here we discuss the evolution for one case in detail ($m_{\rm atm} \simeq 0.008\ M_\odot$) and describe the differences in the other cases as appropriate.

The initial setup of our model is shown in Fig. 1(a). The W7 ejecta occupies the innermost region of the grid, shown in shades of red. The yellow ellipsoidal region surrounding the ejecta represents material expelled during the deflagration. The black contour lines enclose the regions where the calcium number abundance exceeds 1%. In particular, the contour in the top portion of the image marks calcium produced in the deflagration; the inner calcium-rich ring is that of the W7 nucleosynthesis.

The overall hydrodynamic evolution in our model is best described as ejecta impacting a stratified atmosphere, with shock-related effects playing a minor role. In Fig. 1(b) ($t = 0.3$ s), a mostly spherical expansion of the supernova shock can be seen in the lower part of the computational domain. In the upper part of the domain, the ejecta impacts and deforms the extended atmosphere. By $t = 1.24$ s (Fig.1(c)), that impact has lead to the compression of the calcium-rich material into a pancake-like structure of radius $\sim 30,000$ km, located near $z \approx 2 \times 10^9$ cm. By that time, the ambient medium surrounding the atmosphere has been completely overrun by the forward supernova shock. The reverse shock can be seen as the highly contrasted spherical structure starting at $(r, z) = (0, -2.6 \times 10^9)$ cm.

Beginning at $t \approx 1$, the overall expansion becomes in-

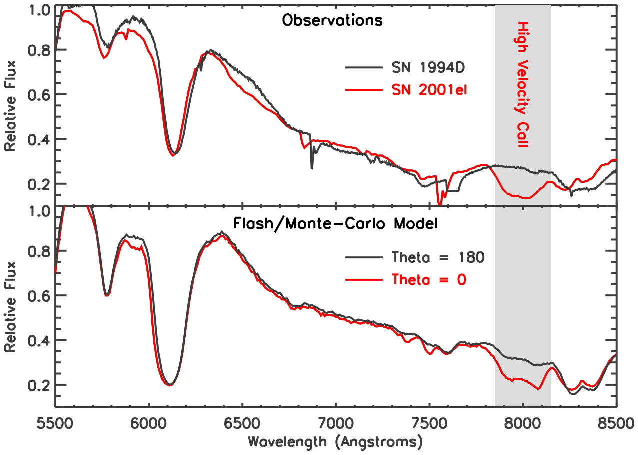

FIG. 2.— Comparison of the synthetic model spectra to Type Ia supernova observations. Top panel: Spectral observations of two Type Ia SNe near maximum light; SN 2001el (red line, Wang et al. 2003) shows a strong HV calcium absorption at 8000 Å while SN 1994D (black line, Patat et al. 1996) does not. Bottom panel: Synthetic model spectra at 20 days. A HV calcium absorption is clearly seen when looking straight down on the calcium-rich pancake (viewing angle $\theta = 0°$, red line), whereas none is seen from the opposite side ($\theta = 180°$, black line).

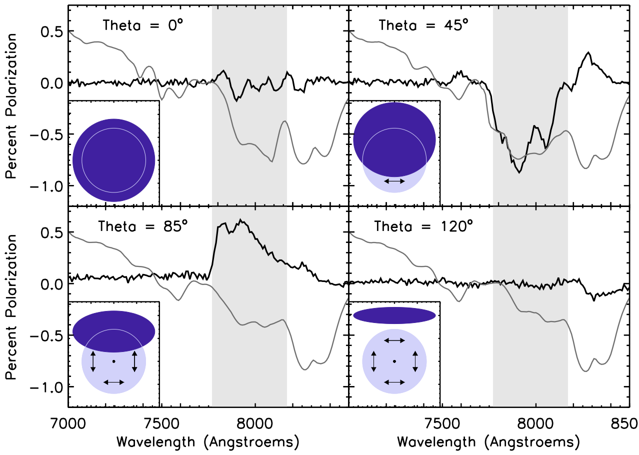

FIG. 3.— Synthetic polarization spectra of the model at 20 days. By convention, a positive (negative) polarization level signifies polarization aligned parallel (perpendicular) to the symmetry axis. The black lines show the polarization level while the gray lines show the corresponding (arbitrarily scaled) flux spectrum. The insets illustrate how the HV calcium line polarization is caused by the partial obscuration of the supernova photosphere (light blue disk) by the calcium-rich pancake (dark blue object).

creasingly homologous, and we stop our calculation at $t = 1.24$ s. Fig. 1(d) shows the total velocity in the upper portion of the computational domain at the final time. The calcium-rich pancake structure shows a significant velocity gradient across its body ($\Delta v/c \approx 0.02$). The central region of the pancake ($r = 0$) moves with velocity spanning 17,000-24,000 km s^{-1}, while near the outer rim the velocity is higher (22,000-28,000 km s^{-1}).

In the case of a more massive atmospheres, the overall evolution and resulting morphology are similar to the case described above. The major difference is the final velocity of the calcium-rich pancake. For a model with $m_{\mathrm{atm}} = 0.016\ M_{\odot}$, the inner part of the pancake moves with velocities 14,000-20,000 km s^{-1}, while the outer edge moves at 21,000-26,000 km s^{-1}. For an even more massive atmosphere ($m_{\mathrm{atm}} = 0.08\ M_{\odot}$) the velocities are still lower, increasing from 10,000-12,000 km $\mathrm{s}^{-1}$to 17,000-21,000 km s^{-1}across the pancake. In this case the calcium-rich pancake almost overlays the region of intermediate mass elements in the W7 ejecta.

The synthetic spectrum of the model at a time when the supernova is near maximum light has been obtained after homologously expanding the ejecta to 20 days (lower panel of Fig. 2). Given the enhanced abundance of intermediate mass elements and relatively low temperature ($T \approx 5500$ K), the pancake is opaque in the Ca II IR triplet lines. For a viewing angle, θ, in which the observer looks directly down upon the pancake ($\theta = 0°$), the pancake obscures the supernova photosphere, creating a broad and highly blueshifted HV calcium absorption feature near 8000 Å. The HV feature seen in the model compares well to that observed in SN 2001el (Wang et al. 2003), shown in the top panel of Fig. 2. For larger viewing angles, the pancake obscures less (or none) of the photosphere, and the HV feature is weaker or absent in the model spectrum. This orientation effect may explain why in some supernovae, such as SN 1994D (Patat et al. 1996), a HV calcium feature at maximum light is seen only weakly or not at all.

The aspherical geometry of the calcium-rich pancake also leads to significant polarization over the HV calcium feature (Fig. 3). Light in the supernova ejecta becomes polarized by electron scattering. By convention, a positive (negative) polarization level signifies polarization oriented parallel (perpendicular) to the symmetry axis. Because the electron-scattering photosphere in our model is essentially spherical, the observed polarization cancels in the continuum. However, the HV pancake may partially obscure the underlying photosphere, leading to a non-zero polarization over the HV calcium feature. This effect is illustrated by the insets to Fig. 3.

The line polarization created in this way depends sensitively upon the viewing angle. For $\theta = 0°$, the polarization cancels completely due to the azimuthal symmetry (Fig. 3(a)). As θ is increased, the absorber selectively reveals horizontally polarized light from the lower rim of the photosphere, resulting in negative line polarization of order $\sim 1\%$ (Fig. 3(b)). For $\theta = 45°$, the model closely reproduces the HV line polarization peak observed in SN 2001el (Wang et al. 2003). For larger θ, vertically polarized light from the side edges of the photosphere dominates, and the line polarization changes sign (Fig. 3(c)). For $\theta \gtrsim 110°$, the pancake no longer obscures the photosphere, and leaves no obvious signature in either the flux or polarization spectrum (Fig. 3(d)).

4. DISCUSSION

We have demonstrated that the observations of a peculiar HV calcium feature in Type Ia supernovae are naturally explained within the GCD model. In the model, burned material expelled during the breakout of the deflagrating bubble forms an extended atmosphere above the stellar surface. That atmosphere is subsequently compressed and accelerated during the hydrodynamic interaction with the supernova ejecta. This leads to the formation of a high-velocity calcium-rich pancake with cross-section comparable to that of the underlying photosphere. The partial obscuration of the photosphere by the pancake results in a HV calcium absorption feature with significant line polarization.

In our model, the blueshift of the absorption feature depends sensitively upon the mass of the expelled material. For the fiducial case studied here ($m_{\rm atm} = 0.008\ M_\odot$), the pancake material spans the velocity range 17,000-24,000 km $\rm s^{-1}$, and is geometrically detached from the bulk of the supernova ejecta. This compares well with the velocities inferred from the HV calcium feature of SN 2001el. As the atmosphere mass is increased, the absorbing pancake moves at lower velocity and eventually blends with the region of intermediate mass elements in the supernova ejecta. In such a case we might expect a very different observable signature, in which the pancake material increases the strength and blueshift of several of the normal Type Ia spectral features. This could provide an orientation-dependent explanation for the unusually high velocities and peculiar velocity evolution of the normal features in some Type Ia SNe (e.g., SN 1984A (Branch 1987) and SN 2002bo (Benetti et al. 2004)).

The large size of the absorbing pancake results in the distinctive orientation effects present in our model. The strength of the HV flux absorption depends only upon the fraction of the photosphere obscured by the pancake, and hence decreases monotonically with θ. The line polarization, in contrast, is maximal when either a large or a small part of the photosphere is covered. Such behavior could be tested with a large sample of spectropolarimetric observations of SNe Ia; in particular, one could study the correlation between the HV calcium polarization level with the depth of the flux absorption.

Although the HV calcium feature is the most profound signature of the absorbing pancake, the opacity due to numerous iron and titanium lines creates a modest flux depression in the wavelength region 3500-4500 Å. This leads to a variation of the B-band magnitude with viewing angle of order one tenth of a magnitude. As discussed in Branch et al. (2004) and Thomas et al. (2004), the temporal evolution of this opacity should also affect the shape of the supernova light curve. Therefore, the presence of the calcium-rich absorber is another intrinsic source of SNe Ia photometric diversity, of possible relevance to their cosmological application.

The presence of a HV calcium absorber can possibly be explained in other explosion scenarios. For example, the large bubbles of burned material present in the pure deflagration and standard DDT models may in principle produce a number of HV absorbers. This case can be distinguished from the case of single absorber in the GCD model using a rich sample of spectropolarimetric observations. In particular, our model predicts a much smaller fraction of supernovae showing a persistent HV calcium feature, as well as the aforementioned polarization correlations. Note that multi-epoch observations may be necessary to separate the signatures of the HV absorber from the "transient ionization" effect discussed by Gerardy et al. (2004), whereby the recombination of Ca III to Ca II in the cold outer layers of ejecta may also give rise to a (short-lived) HV IR triplet absorption in the epochs prior to maximum light.

For several SNe Ia, polarization in the continuum has also been detected, indicating a global asymmetry in the bulk of the supernova ejecta. In SN 2001el, the continuum polarization angle differed from that of the HV calcium feature, suggesting that the orientation of the HV absorber deviated from that of the ejecta. One possible explanation for this difference is that the ejecta acquired a separate, large-scale asymmetry due to the interaction with a companion star (Marietta et al. 2000; Kasen et al. 2004). Another interesting possibility is to consider the GCD framework with rotation of the progenitor included. In such a case, the trajectory of the buoyantly rising deflagrating bubble is not expected to be aligned with the rotation axis of the progenitor. This lack of correlation follows from the fact that the convective core of the white dwarf is expected to produce ignition seed points in a largely stochastic manner. Such a scenario should be studied in the future by means of integrated multi-dimensional hydrodynamical simulations.

We thank Lifan Wang for use of the spectra of SN 2001el, Rollin Thomas for collaborating in the development of the radiative transfer techniques, and the anonymous referee for helpful comments. This work is supported in part by the U.S. Department of Energy under Grant No. B523820 to the Center for Astrophysical Thermonuclear Flashes at the University of Chicago. DK acknowledges support from a NASA ATP grant. This research used resources of the National Energy Research Scientific Computing Center, which is supported by the Office of Science of the U.S. Department of Energy under Contract No. DE-AC03-76SF00098.

REFERENCES

Arnett, D. W. 1969, Ap&SS, 5, 180
Benetti, S. et al. 2004, MNRAS, 348, 261
Branch, D. 1987, ApJ, 316, L81
Branch, D. et al. 2004, ApJ, 606, 413
Fryxell, B. et al. 2000, ApJS, 131, 273
Gamezo, V. N., Khokhlov, A. M., & Oran, E. S. 2004, PRL, 92, 211102
Gerardy, C. L. et al. 2004, ApJ, 607, 391
Höflich, P. et al. 2002, ApJ, 568, 791
Hatano, K. et al. 1999, ApJ, 525, 881
Hillebrandt, W. & Niemeyer, J. C. 2000, ARA&A, 38, 191
Kasen, D. 2004, PhD thesis, University of California, Berkeley
Kasen, D. et al. 2003, ApJ, 593, 788
—. 2004, ApJ, 610, 876
Khokhlov, A. 1991, A&A, 245, 114
Khokhlov, A., Müller, E., & Höflich, P. 1993, A&A, 270, 223
Khokhlov, A. M. 2001, ApJ, submitted; astro-ph/0008463
Li, W. et al. 2001, PASP, 113, 1178
Lucy, L. B. 1999, A&A, 344, 282
Marietta, E., Burrows, A., & Fryxell, B. 2000, ApJS, 128, 615
Nomoto, K., Thielemann, F., & Yokoi, K. 1984, ApJ, 286, 644
Patat, F. et al. 1996, MNRAS, 278, 111
Plewa, T., Calder, A. C., & Lamb, D. Q. 2004, ApJ, 612, L37
Reinecke, M., Hillebrandt, W., & Niemeyer, J. C. 2002, A&A, 391, 1167
Thomas, R. 2003, PhD thesis, University of Oklahoma
Thomas, R. C. et al. 2004, ApJ, 601, 1019
Wang, L. et al. 2003, ApJ, 591, 1110